Combustion Synthesis of Doped $LaGaO_3$ Perovskite Oxide with Fe

Feng-Fan Hsieh, Noriyuki Okinaka and Tomohiro Akiyama

Center for Advanced Research of Energy Conversion Materials, Hokkaido University

Kita 13 Nishi 8, Kita-ku, Sapporo 060-8628, Japan

Corresponding author Answer1 Tel.: +81 11 706 6842; fax: +81 11 726 0731.

E-mail address: halaumi @yahoo.com.tw (Feng-Fan Hsieh).

Abstract

$La_{0.7}Sr_{0.3}Ga_{0.7}Mg_{0.1}Fe_{0.2}O_{3-\delta}$ (LSGMF73712) has been proposed as a new substitute for solid electrolyte in SOFC (solid oxide fuel cells). It has several merits, such as lower operating temperature of SOFC, high transport number of oxide ion and higher electronic conductivity. In this study, the doped-lanthanum gallium with Fe was produced by combustion synthesis, and the effect of particle sizes on sintering behaviors of La(Sr)Ga(Mg)$FeO_{3-\delta}$ samples by spark plasma sintering (SPS) was analyzed by comparing with the traditional solid-state reaction method.

In the experiments of the combustion synthesis, lanthanum oxide, strontium carbonate, metallic gallium, pure iron, metallic magnesium and sodium perchlorate were mixed uniformly and were ignited at one end of the sample under the argon atmosphere to complete the combustion process without any additional energy. Not only could this method shorten the processing time, but also it could minimize the sintering temperature in the production. As a result, the product showed definite peaks of lanthanum gallium in X-ray diffraction (XRD) patterns and the product could be sintered at a lower temperature 1473 K by SPS method, in comparison to a conventional solid-state reaction method. Moreover, the sintering temperature of the products could further decrease in a lower temperature 1273 K after ball-mill treatment.

Keywords: combustion synthesis; perovskite type oxide; Solid oxide fuel cell (SOFC); $LaGaO_3$; Fe dope; spark plasma sintering (SPS)

1. Introduction

Our planet is threatened with serious environmental challenges, such as global warming and abnormal weather, which are urgently addressed. Solid oxide fuel cells (SOFC) have attracted worldwide attention as clean power generators with high efficiency and have no pollution [1, 2]. Oxide ion conductor plays an important role in SOFC as the electrolyte. The perovskite oxide, which supplies large amount of vacancies [3], can be expected to obtain high oxide ion conductivity. Several studies have shown that perovskite oxide of $LaGaO_3$ doped with Sr and Mg for La and Ga site, respectively, exhibits high oxide ion conductivity [4, 5]. Not only can the $LaGaO_3$-based oxide show high conductivity in the electrolyte, but also it can be used for intermediate-temperature SOFCs [6–10]. In addition, oxide ion conductivity in $LaGaO_3$ doped with Sr and Mg for La and Ga site, respectively, is further increased by doping with transition metal such as Co or Fe [11], and maximum power density of the cell also increases when Co- or Fe-doped $LaGaO_3$ was used for the electrolyte [12-13].

$La_{0.7}Sr_{0.3}Ga_{0.7}Mg_{0.1}Fe_{0.2}O_{3-\delta}$ is reported as a new replacement for solid electrolyte by the sintering method [14], which is highly time requirement and energy consuming. Combustion synthesis (CS) is a well-known method discovered by A.G. Merzhanov and coauthors in 1967 and has been used as a substitute approach to resolve this problem [15, 16, 17]; the merits of CS are the fast response, saving producing time, and no additional input energy during the combustion process. The $LaGaO_3$ product, which doped with Fe and Mg for Ga site, was produced through combustion synthesis instead of the conventional solid-state reaction method. Furthermore, the produced LSGMF73712 ($La_{0.7}Sr_{0.3}Ga_{0.7}Mg_{0.1}Fe_{0.2}O_{3-\delta}$ compositions are denoted by the abbreviation LSGMF73712 in this paper) samples were sintered by using spark plasma sintering (SPS) method and the effect of distinct particle sizes was investigated into the sintering temperature of products. Hence, different ball-mill processing times were required in this investigation. Finally, the processing

time and electric energy consumption in the LSGMF production were assessed by a comparative analysis between the combustion synthesis and the solid-state reaction method.

2. Experimental

2.1. Sample preparation

Fig. 1 shows the comparison of experimental flow between the traditional sintering method and the combustion synthesis manner for producing LSGMF. In the combustion synthesis, when one end of the mixed sample is ignited at the ignition point, the combustion wave transits to the other end completely and the desired composition of the product is gained in short time (see phase 1 in Fig. 1(b)). All specimens used in this study were prepared from calculated powders of La_2O_3 (Aldrich, 99.9 % purity), $SrCO_3$ (Aldrich, 99.9 % purity), metallic gallium powder (High Purity Chemical Co. Ltd., 99.99 % purity), metallic magnesium (High Purity Chemical Co. Ltd., 99.9 % purity), pure iron (High Purity Chemical Co. Ltd., 99.9 % purity) and $NaClO_4$ (Aldrich, 98 % purity).

Table 1 shows the experimental results of diverse mixtures for producing LSGMF and the adiabatic temperature (T_{ad}) of each case has also shown in Table 1. The temperatures were calculated by the following equation:

$$\int_{298}^{Tad} (\sum_i n_i C_{ip}) dT = -\Delta H_r^o \quad (1)$$

Here ΔH_r^o gives a standard enthalpy of reaction and n_i expresses a stoichiometric number of a product (i): $La_{0.7}Sr_{0.3}Ga_{0.7}Mg_{0.1}Fe_{0.2}O_3$, CO_2 (g), NaCl (g), and C_{ip} gives its molar specific heat capacity of the product. Generally speaking, T_{ad} provides an indication of whether or not combustion synthesis (CS) can proceed via the self-propagating mode and has been empirically judged that the CS mode can be sustained

only if $T_{ad} \geqq 1800K$[16]. As seen in case 4, even though the powder mixtures of La_2O_3, $SrCO_3$, Ga_2O_3, Mg, and Fe had been treated with the ball-mill treatment for 72 h before combustion synthesis, the mixed powders could not be ignited at the ignition point. The combustion reaction could proceed successfully when metallic gallium and magnesium were used as alternatives in place of theirs oxide in order to utilize highly exothermic reaction for combustion synthesis (ΔH_r^o = -255 kJ/mol, T_{ad}= 3070 K). In contrast, all raw materials used in the sintering method were oxides. Sodium perchlorate, which could supply the necessary oxygen for a reaction with an appropriate stoichiometric coefficient of products, was chosen as an oxidizing reagent for the combustion process.

Table 1
Experimental result of diverse mixtures for producing LSGMF

Case	Powder 1	Powder 2	Powder 3	Powder 4	Powder 5	Ignition/propagation	T_{ad} (K)
1	La_2O_3	$SrCO_3$	Ga_2O_3	MgO	Fe_2O_3	X/X	1020
2	La_2O_3	$SrCO_3$	Ga_2O_3	Mg	Fe_2O_3	X/X	1450
3	La_2O_3	$SrCO_3$	Ga_2O_3	Mg	FeO	X/X	1610
4	La_2O_3	$SrCO_3$	Ga_2O_3	Mg	Fe	X/X	1580
5	La_2O_3	$SrCO_3$	Ga	Mg	Fe	O/O	3070

2.2. Experimental procedure

Fig. 2 illustrates a schematic diagram of the experimental apparatus used in the CS of LSGMF and this equipment consists of a reactor, a gas supply system, and a vacuum system. The preparation procedure had shown as follows. To begin with, these starting materials were stoichiometrically mixed in an Al_2O_3-ball mill at 30 rad/min for 3 h in air; the alumina milling pot contained alumina balls of 10 mm in diameter. A notable point for attention was that the mixing velocity could not exceed the speed of 30

rad/min because of the low melting point of gallium. Since gallium's melting point (29.76 °C) is near room temperature, gallium will melt in one's hand easily. Liquid gallium metal wets glass and skin, making it mechanically more difficult to handle, even though it is substantially less toxic and required far fewer precautions. Secondly, the powder mixture was placed in a graphite crucible, 20 mm (W) × 30 mm (L) × 7 mm (H), without any compressive treatment, and the weight of this sample was approximately 8 g. Third, the inner air of the reactor was evacuated by a rotary pump for 10 min; subsequently, pure argon was supplied to the atmospheric pressure. Finally, a disposable carbon foil, which is used as an igniter, 5 mm × 200 mm × 0.1 mm, was placed contact with one end of the sample and was electrically flashed at 50 V and 100 A at room temperature. Furthermore, the reaction process, which consists of ignition, self-propagation, and completion, could be observed through the upper glass window of the equipment during the CS.

After the CS, the samples were treated with a planetary ball-mill treatment; the stainless steel milling pot contained stainless steel balls of 10 mm in diameter. The synthesized product and the stainless steel balls were simultaneously put into the pot, and the container was set in the ball-mill apparatus and milling condition was carried out at a rotation rate of 300 rpm with a powder-to-ball mass ratio of 10:1 in air. Ball-milled samples were obtained after milling for 10, 30, 50, and 70 h respectively. The ball-milled products were also observed by scanning electron microscopy (SEM) for analyzing the microstructure, and the products were identified by X-ray diffraction (XRD) analysis. Compared the results of XRD with the ones obtained from the SSM,

the lattice parameters could be calculated on the basis of several sharp peaks over a wide range of diffraction angles. In addition, the average particle-size distributions of the ball-milled products were also investigated by laser-scattering particle-size distribution analyzer (HORIBA, LA-950), in which water was used as a dispersing fluid. In the spark plasma sintering (SPS) procedure, the no ball-milled samples (5 g) were pressed into a disk (15 mm in diameter) at 30 MPa and the samples were sintered at different constant temperatures from 1273 K to 1673 K for 1.5 h in vacuum for determining the optimum sintering temperature. By contrast, the samples were sintered at 1773 K for 6 h at 70 V and 12 A in air by solid-state reaction method (see phase 2 in Fig. 1(a)).

3. Results and discussion

3.1. Combustion synthesis (CS) of LSGMF73712

The samples emitted plenty of exothermal heat and white smoke during the CS in the case 5 (Table 1). White smoke generation was likely owing to the evaporation of sodium chloride. The reaction in the case 5 was caused by the following the overall exothermic reaction (2):

$$0.35La_2O_3+0.3SrCO_3+0.7Ga+0.1Mg+0.2Fe+0.4125NaClO_4 \rightarrow$$

$$La_{0.7}Sr_{0.3}Ga_{0.7}Mg_{0.1}Fe_{0.2}O_3+0.3CO_2\,(g)+0.4125NaCl\,(g) \quad (2)$$

However, the samples were not successfully ignited during the CS in the cases 1, 2, 3 and 4 (Table 1) due to weak exothermic reaction of very small magnesium despite of ignition.

3.2. Ball-mill treatment

Fig. 3 shows the photographs of the ball-milled samples with different ball-milling time before and after SPS. The colors of the combustion-synthesized products changed from light brown to brown after the ball-mill treatment, and the specimens presented the distinct colors with diverse milling time from 0 to 70 h before SPS. However, the color of SPSed samples changed into black after SPS. As shown in Table 2, the average particle size of the LSGMF73712 product with no ball-mill treatment was approximately 12.7 μm and the particle sizes decreased with increasing the ball-milling time; still, the ball-milled sample for 70 h was approximate to 4.6 μm. This phenomenon may be explained by the high surface energy of extremely fine powders.

Fine powders tend to agglomerate into larger entities easily and achieve some reduction in surface energy. The agglomerates are particle clusters and are influenced apparently by the surface energy.

Table 2
Average particle size of the CSed products with different ball-mill processing time for preparing LSGMF samples

Case	Processing time (hour)	Temperature and atmosphere	Average particle size (μm)
1	0 h	Room temperature in the air	12.7
2	10 h		5.3
3	30 h		4.4
4	50 h		3.2
5	70 h		4.6

Fig. 4 shows SEM micrographs of the LSGMF73712 samples, in comparison to the ball-milled one for 70 h. The apparent difference between two pictures shows that grains of the ball-milled sample with 70 h were cohering partly. The extremely small particles cohered into agglomerates easily because the cohesion united particles of the same material. Therefore, it is considered that the excessive ball-milling time is not advantageous to fine the grains of the LSGMF73712 samples.

3.3. XRD phase analysis

Fig. 5 shows the XRD patterns of the products after the CS at argon atmosphere with different ball-milling time. The second phase lanthanum strontium gallium oxide ($LaSrGaO_4$) and the main phase of $LaGaO_3$ perovskite were observed on the XRD pattern of $LaGaO_3$-based oxide doped with Fe, but no diffraction peak from an oxide

containing Fe was observed. The valence number of the doped Fe at the Ga site in the perovskite lattice was trivalent，but $LaSrGaO_4$ was not similar to a perovskite type oxide.

Table 3
Estimated ratios of the lattice parameter of the ball-milled LSGMF73712.

Ball-milling time	**Lattice parameter ratio /-**	
	a/b	c/b
LSGMF-BM 70h	0.9995	1.0005
LSGMF-BM 50h	0.9995	0.9987
LSGMF-BM 30h	0.9992	0.9938
LSGMF-BM 10h	0.9995	0.9988
LSGMF-BM 0h	0.9998	1.0037
$LaGaO_3$*	0.994	1.40

* Reference data, obtained from JCPDS card.

Table 3 shows the estimated lattice parameter ratios of ball-milled products that are produced in each case. The reference data for lanthanum gallate ($LaGaO_3$) of SSM are also listed. The crystal structure of lanthanum gallate-based perovskite oxide is known to be orthorhombic (Pb *nm*) at room temperature [19]. However, perovskite oxide with cubic structure seems to be stabilized by doping Fe for Ga site. In doping magnesium and iron at the gallium site, the origin of the dopant effect of Fe can release the local stress in the lattice because the ionic size of Fe^{3+} (64 pm) is intermediate between Ga^{3+} (62 pm) and Mg^{2+} (66 pm). Consequently, we conclude that doping larger sized cation of Fe^{3+} for Ga site may enlarge the lattice constant. The lattice parameter of the produced LSGMF73712 gradually decreased with increasing the ball-milling time up to LSGMF-BM 30 h, and then it increased with increasing the ball-milling time up to

LSGMF-BM 50 h. This may be explained by the cohesion of extremely fine powder. To sum up, the CS successfully produced doped-lanthanum gallate perovskite type oxides LSGMF73712.

Fig. 6 shows the XRD peaks data of the combustion-synthesized products by using different ball-milling time. The percentages of $LaGaO_3$ and mean crystallite size in the ball-milled products have also shown in Fig. 6. It revealed that the peak intensity of the CSed products and the quantity of the second phase $LaSrGaO_4$ gradually decreased with increasing ball-milling time. However, the ratio of intensity to half-peak breadth was enhanced slightly when the CSed product was ball-milled for 70 h. This may be explained by the increase in distance of crystal layers. The relationship between mean crystallite size and the peak broaden effect is shown as following Scherrer equation (3);

$$\beta_{hkl} = K\lambda / (D_{g(hkl)} \cos\theta_{hkl}) \quad (3)$$

where β is the width of the peak at half maximum intensity of a specific phase (hkl) in radians; K is a constant that varies with the method of taking the breadth ($0.89 < K < 1$); λ is the wavelength of incident X-rays; θ is the center angle of the peak (diffraction angle); D_g is the mean grain size of a specific phase of a material. The equation relates the peak breadth of a specific phase of a material to the mean crystallite size of that material. Therefore, it is the quantitative equivalent of saying that the larger a material's crystallites were, the sharper its XRD peaks would be in the CSed powder with ball-milling time for 70 h.

3.4. Sintering behavior of LSGMF73712 sample

Fig. 7 shows the comparison of XRD patterns of the produced samples after spark plasma sintering (SPS) and the reference data for LSGMF after the sintering by SSM was also listed. The peaks of the sample ball-milled for 10 h agreed with those at 1773 K by the SSM. However, the main phase of lanthanum gallate in CSed samples gradually decreased with increasing ball-milling time after SPS. On the contrary, the peaks of the second phases, $LaSrGaO_4$ and $LaSrGa_3O_7$, increased apparently and were observed at samples sintered at 1273 K by the SPS. This may be explained by the volatilization of Ga element in $LaGaO_3$. The Ga atoms in extremely fine powder were easy to volatilize due to the reduction reaction in high temperature. Because the fine particle size brought about the effect of non-stoichiometric ratio in $LaGaO_3$, so the degrees of long-range order and the crystallinity of $LaGaO_3$ were reduced by the effect. In the meantime further increase in the quantity of the second phases was obvious and caused the purity of LSGMF73712 to decline significantly.

The ball-milled samples could be sintered successfully at 1273 K for 40 min (2.5 V and 540A) in vacuum (see phase 2 in Fig. 1(b)). However, the same temperature was not enough for sintering the sample in the SSM and the no ball-milled CSed sample was sintered at 1473 K for 1.5 h (3 V and 600 A) by the SPS. The sintering time of the combustion-synthesized samples were predicted by Herring's Scaling Law [20] and the following equation (4):

$$t_b=(r_b/r_s)^n \cdot t_s \quad (4)$$

In the equation (4), t_s and t_b are the sintering time of small and big particle powder, respectively; r_s and r_b are the radii of small and big particle powder, respectively. According to the law, we judged that fine LSGMF73712 powders could be sintered in a shorter time, in comparison to big particle powder at the same temperature. This may be explained by the high surface energy of fine powder. Because the driving force for sintering of fine LSGMF73712 powder was higher than that of big particle powder. Moreover, the moving distance of atomic diffusion at grain boundaries in fine LSGMF73712 powder was short. The surface energy in specific surface area of ball-milled samples increased with increasing ball-milling time, but the excessive milling time (> BM 50 h) caused the phenomenon of agglomeration in fine powder and the sintering time was extended. Therefore, the appropriate BM treatment can reduce the sintering temperature and time in the SPS process apparently. In addition, based on Archimedes method using ethanol, the relative density of the pellet after sintering by SPS was about 98 % which as the same as the one prepared by SSM.

4. Conclusions

The combustion synthesis (CS) of LSGMF was experimentally studied in comparison to the traditional SSM (solid-state method). The conclusions were derived as follows:

(1) The sample of LSGMF73712 was successfully produced by the combustion synthesis at argon atmosphere and room temperature, in which oxidation heat of metallic gallium and magnesium were effectively used for sustainable reaction.

(2) The peaks of the sample ball-milled for 10 h (SPSed LSGMF73712 BM 10 h) agreed with those at 1773 K by the SSM. However, the excessive ball-mill treatment (>BM 10 h) caused the purity of LSGMF73712 to decline significantly after SPS.

(3) The LSGMF73712 CS-product could be sintered at 1473 K for 1.5 h by the SPS. Owing to smaller size of the powder with the perovskite phase than the SSM's one after ball-mill treatment, the sintering temperature drastically lowered to 1273 K (sintering time = 40 min) by 500K, in comparison to the SSM.

According to the above point of views, we conclude that the CS is very beneficial for producing a Fe-doped $LaGaO_3$ electrolyte in the intermediate-temperature SOFC system and spark plasma sintering is also an effective method to sinter the LSGMF electrolyte.

References

[1] M.Q. Minh, T. Takahashi, Science and Technology of Ceramic Fuel Cells, Elsevier, Amsterdam, 1995.

[2] S.C. Singhal, K. Kendal, High Temperature Solid Oxide Fuel Cells: Fundamentals, Design and Application, Elsevier, Oxford, 2002.

[3] T. Takahashi, H. Iwahara, Energy Convers. 11 (1971) 105.

[4] T. Ishihara, H. Matsuda, Y. Takita, J. Am. Chem. Soc. 116 (1994) 3801.

[5] T. Ishihara, H. Matsuda, Y. Takita, Solid State Ionics 79 (1995) 147.

[6] M. Feng, J.B. Goodenough, Eur. J. Solid State Inorg. Chem. 31 (1994) 663.

[7] J. Drennan, V. Zelizko, D. Hay, F.T. Ciacchi, S. Rajendran, S.P.S. Badwal, J. Mat. Chem. 7 (1997) 79.

[8] H. Yokokawa, N. Sakai, T. Horita, K. Yamaji, Fuel Cell 1 (2001) 117.

[9] Z.G. Bi, B.L. Yi, Z.W. Wang, Y.G. Dong, H.J. Wu, Y.C. She, M.J. Cheng, Electrochem. Solid-State Lett. 7 (2004) A105.

[10] S. Kanazawa, T. Ito, K. Yamada, T. Ohkubo, Y. Nomoto, T. Ishihara, Y. Takita, Surf. Coat. Technol. 169–170 (2003) 508.

[11] T. Ishihara, H. Furutani, M. Honda, T. Yamada, T. Shibayama, T. Akbay, N. Sakai, H. Yokokawa, Y. Takita, Chem. Mater. 11 (1999) 2081.

[12] T. Ishihara, T. Shibayama, M. Honda, H. Nishiguchi, Y. Takita. J. Electrochem. Soc. 147 (2000) 1332.

[13] T. Ishihara, T. Shibayama, H. Nishiguchi, Y. Takita, J. Mater. Sci. 36 (5) (2001) 1051.

[14] T. Ishihara, M. Ando, M. Enoki, Y. Takita. J. Alloys Comp. 408–412 (2006) 507–511.

[15] T. Akiyama, Y. Hirai, N. Ishikawa, Mater. Trans. 42 (2001) 460.

[16] Z. A. Munir, Am. Ceram. Soc. Bull. 67 (2) (1998) 342-349.

[17] Merzhanov, A.G., Combustion: New Manifestation of an Ancient Process, Chemistry of Advanced Mater. Rao, C.N.R., Ed., Oxford: Blackwell (1992) 19-39.

[18] H. Ishikawa, M. Enoki, T. Ishihara, T. Akiyama, Mater. Trans. 147 (2006) 149-155.

[19] Y. Wang, X. Liu, G.D. Yao, R.C. Liebermann, M. Dudley, Mater. Sci. Eng. A 132 (1991) 13-21.

[20] C. Herring, Effect of Change of Scale on Sintering Phenomena, J. Appl. Phys. 21 (1950) 301.

Caption List

Figure 1: Comparison of experimental flow between the traditional sintering method and proposed one for producing La(Sr)Ga(Mg)FeO_3. Metallic gallium, magnesium and sodium perchlorate are used for exothermic reaction.

Figure 2: Schematic diagram of the experimental apparatus used for the combustion synthesis in this study.

Figure 3: Photographs of the ball-milled samples with different ball-milling (BM) time before and after SPS

Figure 4: SEM micrographs of the LSGMF73712 electrolytes prepared by different ball-milling time: (a) No ball-mill treatment after combustion synthesis and (b) ball-mill treatment for 70 hours.

Figure 5: XRD patterns of the combustion-synthesized products with different ball-milling time.

Figure 6: XRD peaks data of the combustion-synthesized products by using different ball-milling time.

Figure 7: Comparison of XRD patterns of the produced samples after spark plasma sintering. Asterisk (*) implies the reference data of the sample which obtained by the solid-state method.

Table 1: Experimental results of diverse mixtures for producing LSGMF

Table 2: Average particle size of the CSed products with different ball-mill processing time for preparing LSGMF samples

Table 3: Estimated ratios of the lattice parameter of the ball-milled LSGMF73712.

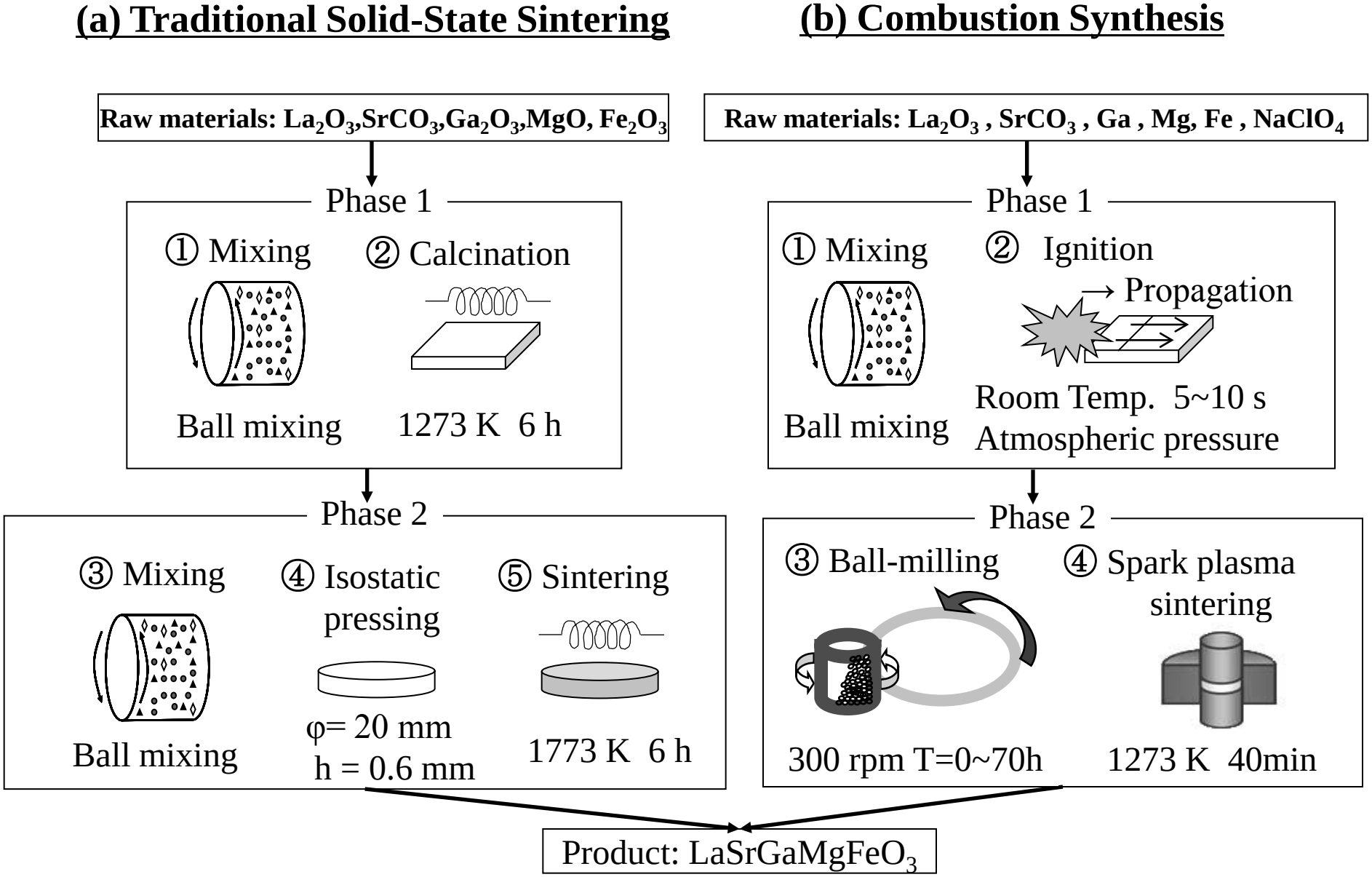

Figure 1 Comparison of experimental flow between the traditional sintering and proposed one for producing La(Sr)Ga(Mg)FeO_3. Metallic gallium, magnesium and sodium perchlorate are used for exothermic reaction [18].

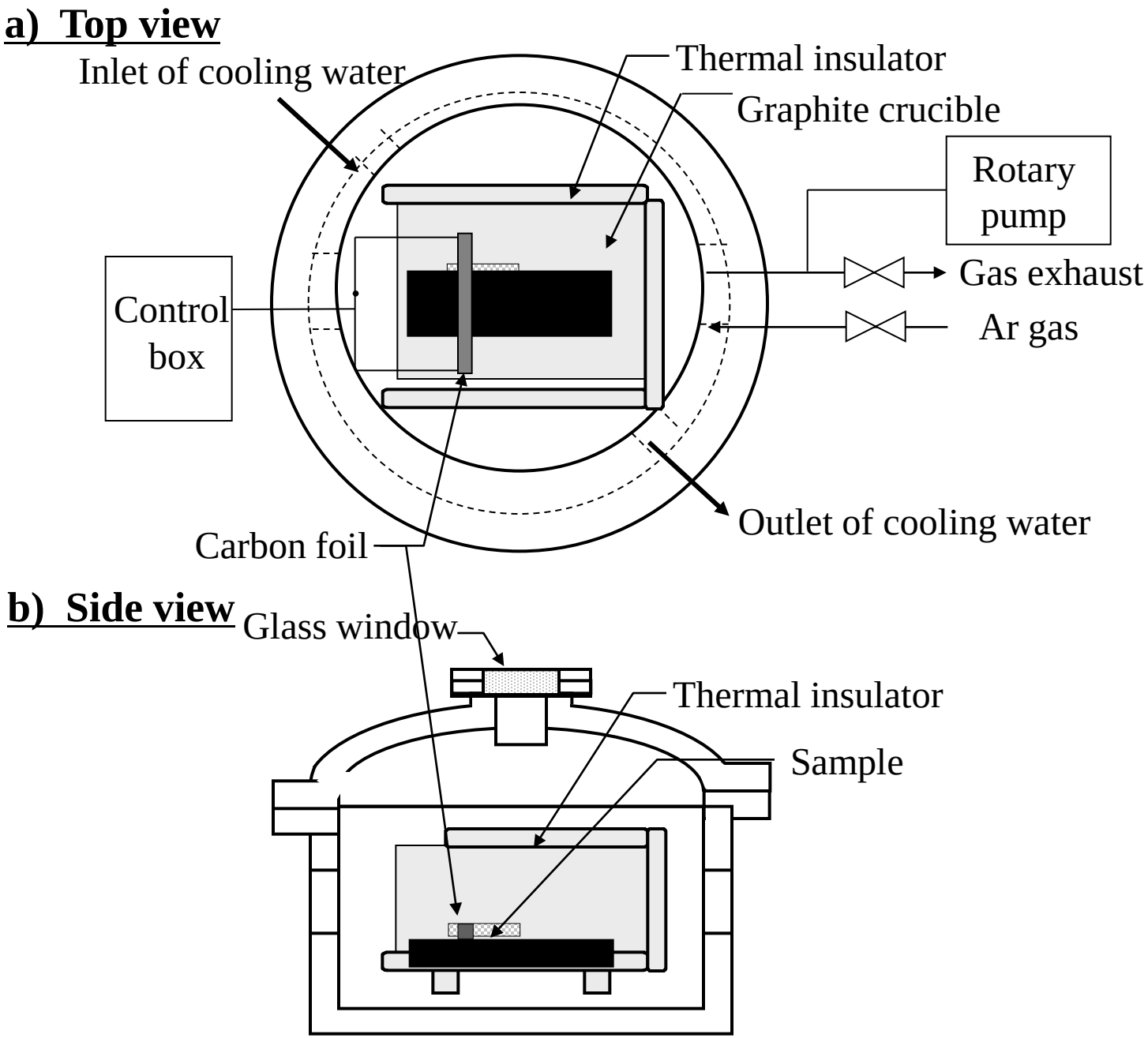

Figure 2 Schematic diagram of the experimental apparatus used for the combustion synthesis in this study [18].

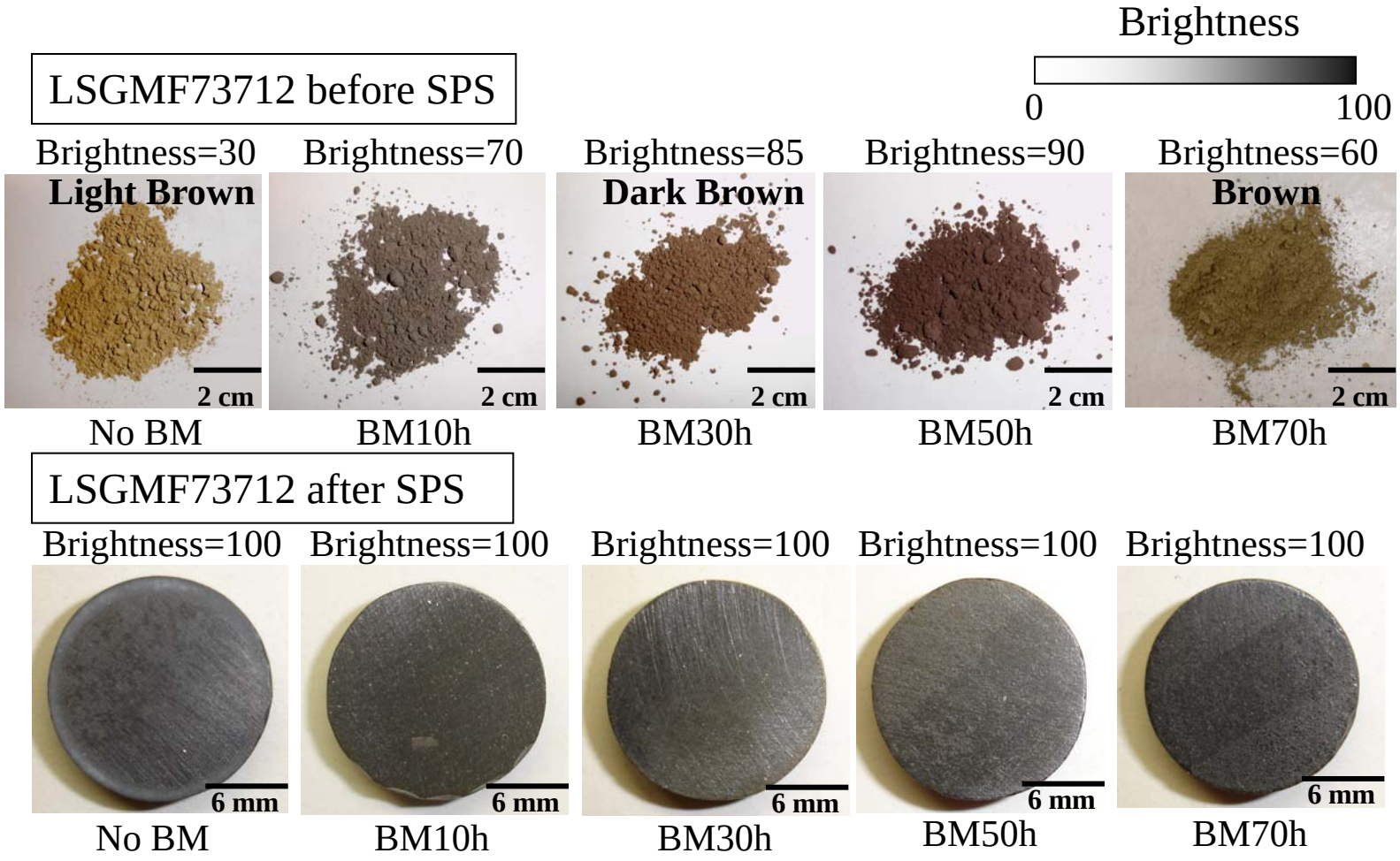

Figure 3 Photographs of the ball-milled samples with different ball-milling (BM) time before and after SPS.

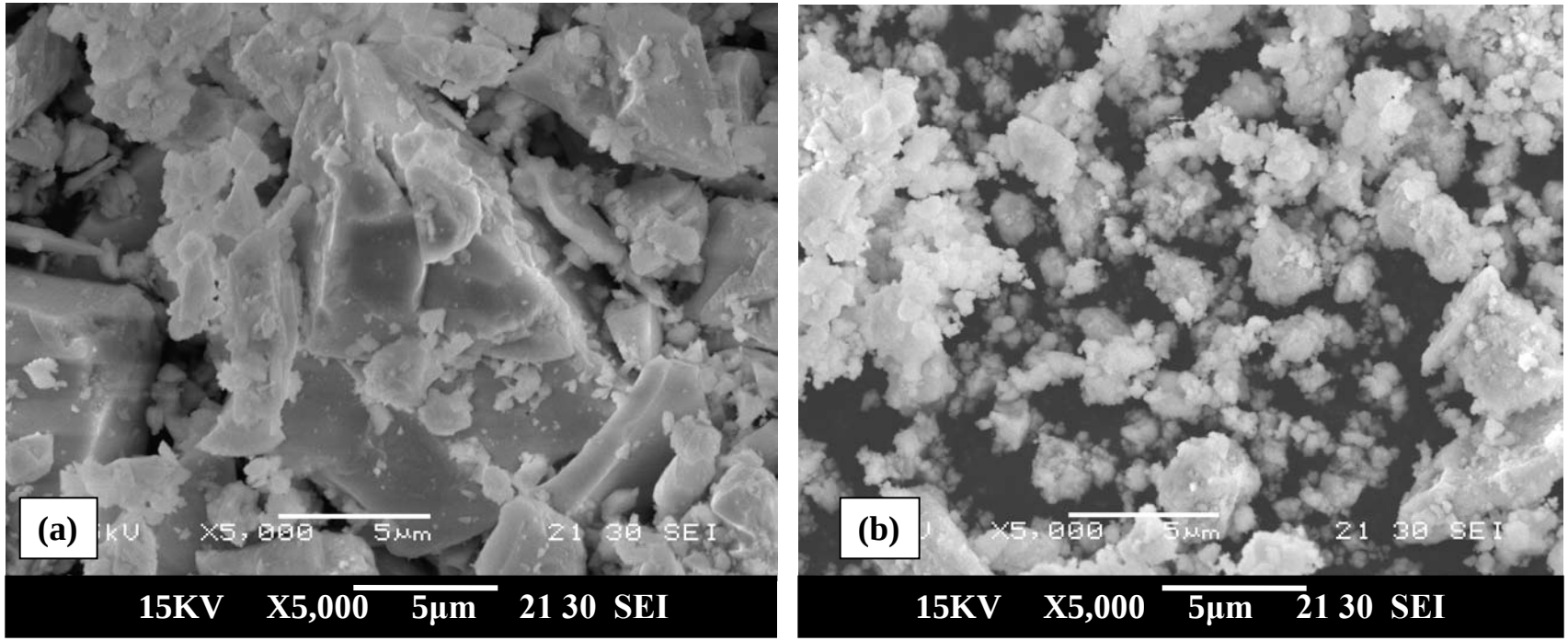

Figure 4 SEM micrographs of the LSGMF73712 electrolytes prepared by different ball-milling time: (a) no ball-mill treatment after combustion synthesis and (b) ball-mill treatment for 70 hours.

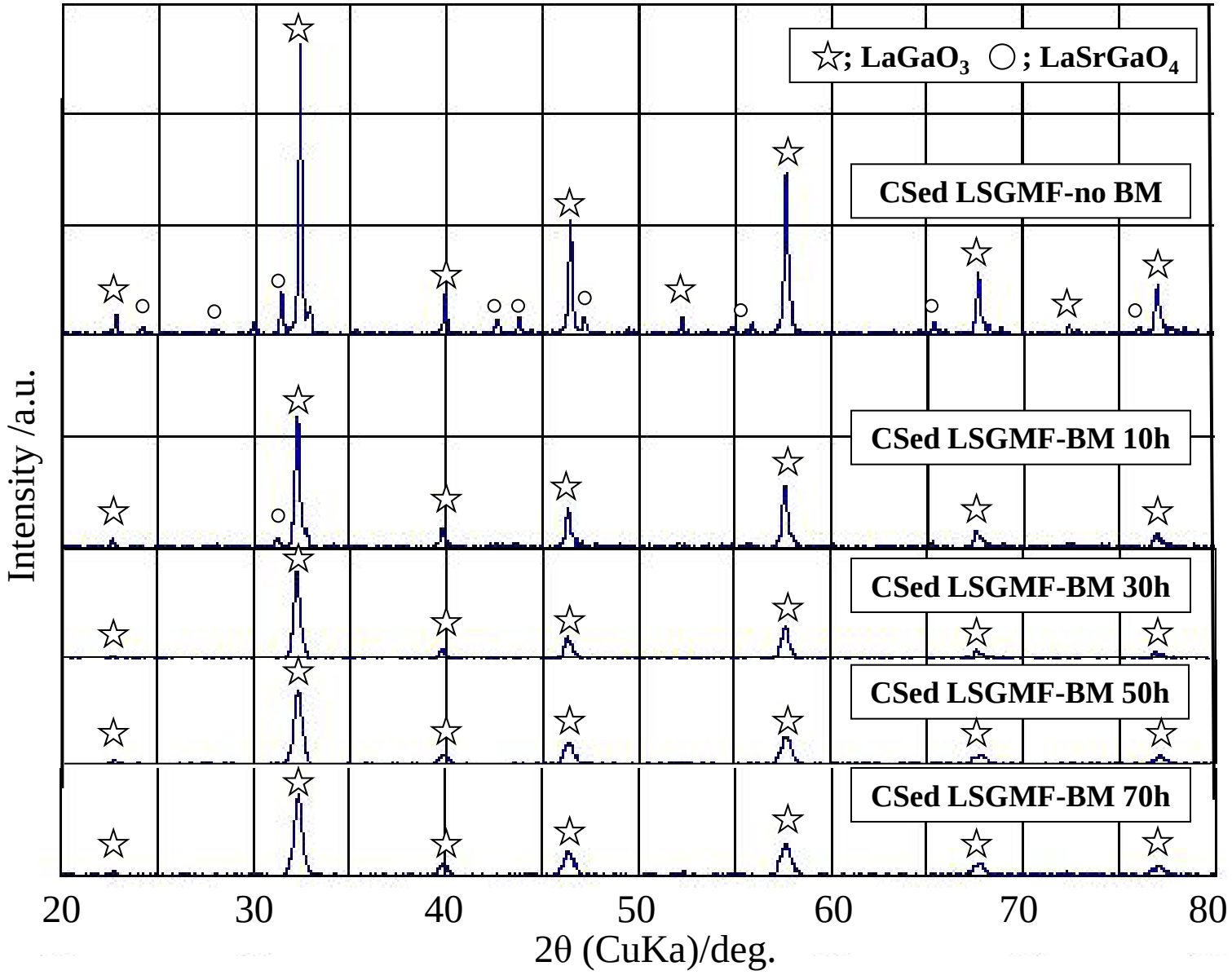

Figure 5 XRD patterns of the combustion-synthesized products with different ball-milling time.

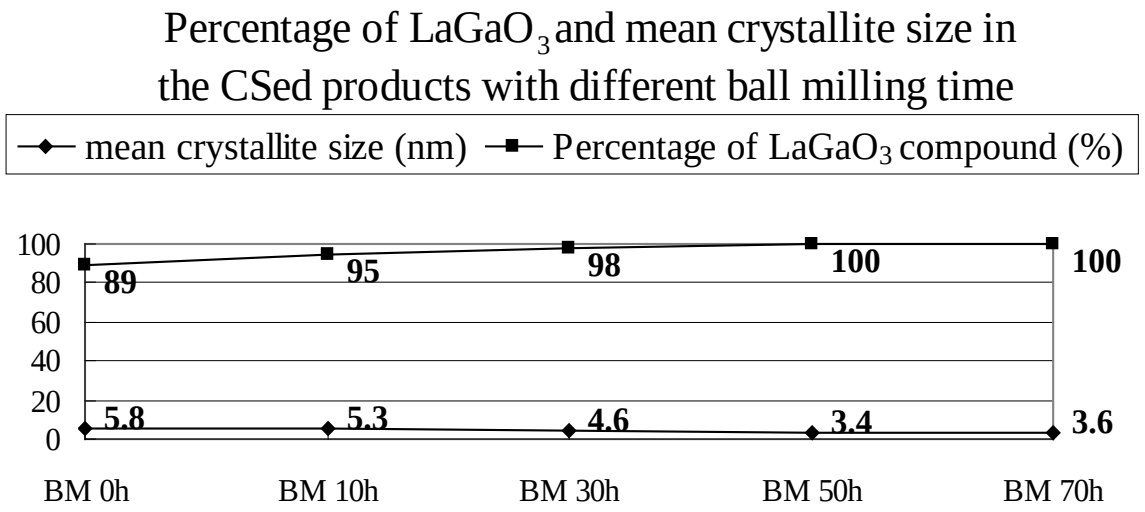

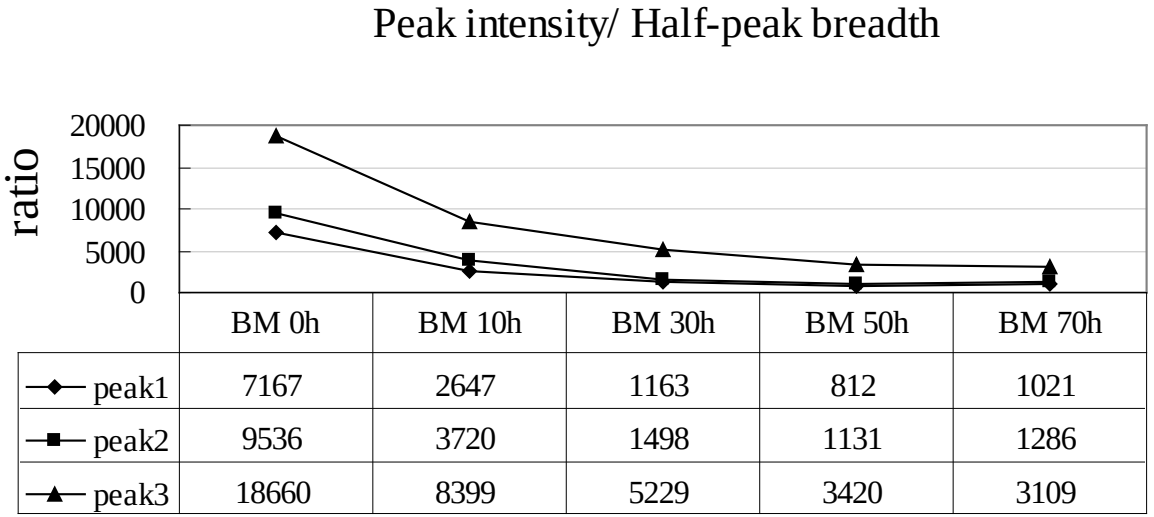

	BM 0h	BM 10h	BM 30h	BM 50h	BM 70h
peak1	7167	2647	1163	812	1021
peak2	9536	3720	1498	1131	1286
peak3	18660	8399	5229	3420	3109

Figure 6 XRD peaks data of the combustion-synthesized products by using different ball-milling time.

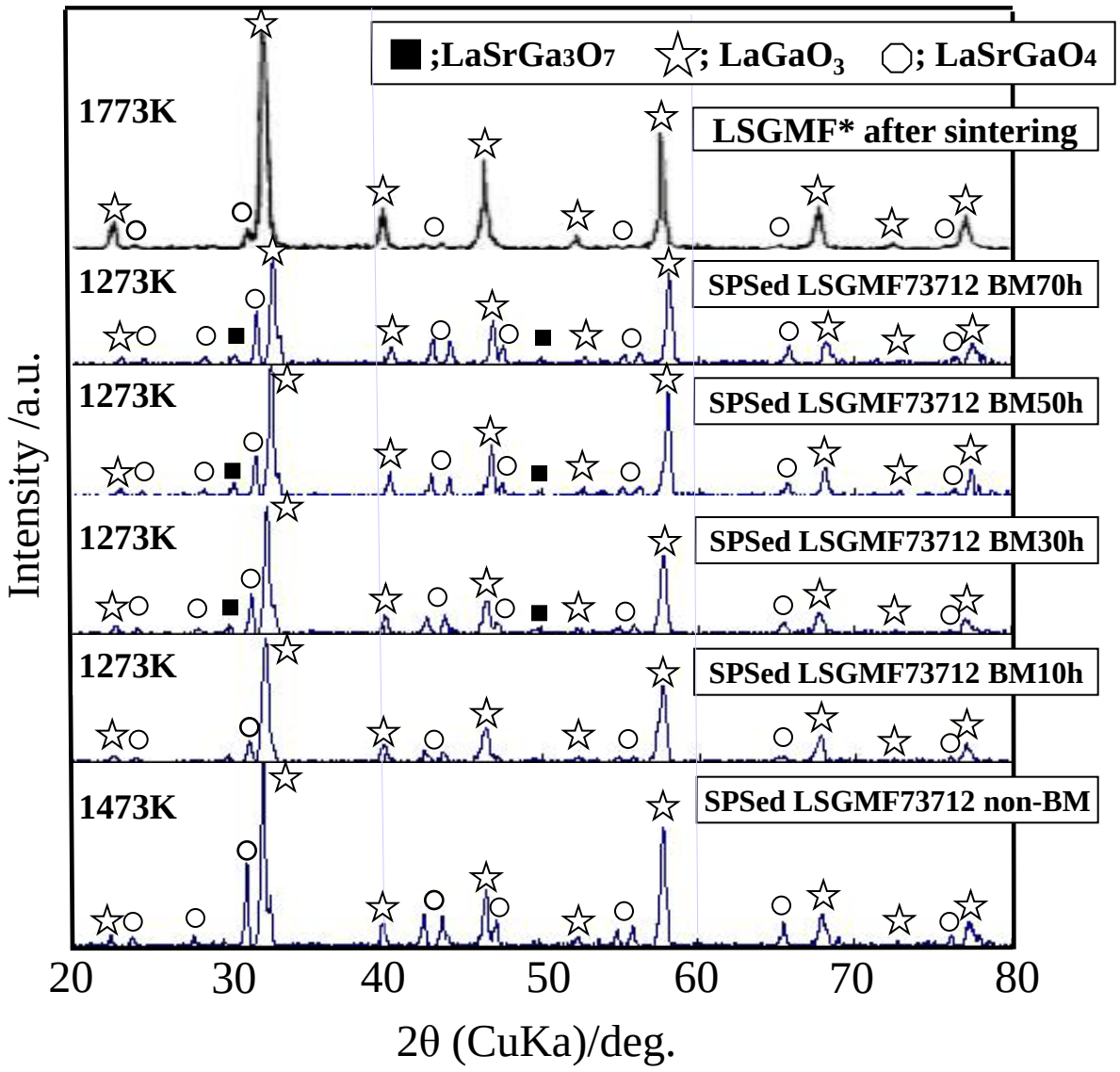

Figure 7 Comparison of XRD patterns of the produced samples after spark plasma sintering. Asterisk (*) implies the reference data of the sample which is obtained by the solid-state method[12].